REFERENCES

[1] C. W. Song, J. G. Rhee, and S. H. Levitt, "Blood flow in normal tissues and tumors during hyperthermia," *J. Nat. Cancer Inst.*, vol. 64, no. 1, pp. 119–124, Jan. 1980.

[2] W. Müller-Klieser and P. Vaupel, "Effect of hyperthermia on tumor blood flow," *Biorheol.*, vol. 21, pp. 529–538, 1984.

[3] H. H. LeVeen, S. Wapnick, V. Piccone, G. Falk, and N. Ahmed, "Tumor eradication by radiofrequency therapy," *J. Amer. Med. Assoc.*, vol. 235, no. 20, pp. 2198–2200, May 1976.

[4] C. W. Song, M. S. Kang, J. G. Rhee, and S. H. Levitt, "Effect of hyperthermia on vascular function in normal and neoplastic tissues," *Ann. N. Y. Acad. Sci.*, vol. 335, pp. 35–43, 1980.

[5] T. Sugahara and K. Abe, *Hyperthermia—A New Method to Treat the Cancer.* Tokyo, Japan: Magbros, 1984.

[6] C. W. Song, A. Lokshina, J. G. Rhee, M. Patten, and S. H. Levitt, "Implication of blood flow in hyperthermic treatment of tumors," *IEEE Trans. Biomed. Eng.*, vol. BME-31, pp. 9–16, Jan. Jan. 1984.

[7] N. Tsuda, K. Kuroda. and Y. Suzuki, "An inverse method to optimize heating conditions in RF-capacitive hyperthermia," *IEEE Trans. Biomed. Eng.*, vol. 43, pp. 1029–1037, Oct. 1996.

[8] Y. Yamamura and T. Sugimura, *Cancer and Hyperthermia.* Tokyo, Japan: Mejikarubyu-sha, 1987.

[9] H. R. Shibata and L. D. MacLean, "Blood flow to tumors," *Prog. Clin. Cancer*, vol. 2, pp. 33–47, 1966.

[10] P. M. van den Berg, A. T. de Hoop, A. Segal, and N. Praagman, "A computational model of electromagnetic heating of biological tissue with application to hyperthermic cancer therapy," *IEEE Trans. Biomed. Eng.*, vol. BME-30, pp. 797–805, 1983.

[11] Y. Tanaka, T. Hasegawa, T. Murata, S. Sawada, and K. Akagi, "Effect of hyperthermia combined with radiation on normal and tumor microcirculation," in *Fundamentals of Cancer Therapy by Hyperthermia, Radiation, and Chemicals.* Tokyo, Japan: Magbros, 1981, pp. 95–109.

Stochastic Complexity Measures for Physiological Signal Analysis

I. A. Rezek* and S. J. Roberts

***Abstract*— Traditional feature extraction methods describe signals in terms of amplitude and frequency. This paper takes a paradigm shift and investigates four stochastic-complexity features. Their advantages are demonstrated on synthetic and physiological signals; the latter recorded during periods of Cheyne–Stokes respiration, anesthesia, sleep, and motor-cortex investigation.**

***Index Terms*—Approximate entropy, autoregressive (AR) model order, spectral entropy (SE), state-space embedding, stochastic complexity.**

I. INTRODUCTION

Physiological signals have a wide variety of forms. To describe them, traditional feature measures typically extract amplitude and frequency information. This makes comparison of signals which have different bandwidths difficult. In addition, such measures do not allow comparison within subject groups as the absolute frequency of rhythms may differ from person to person, and may depend on other factors such as patient sex and age. Hence, other methods are desirable.

When visually inspecting signals, one of the first impressions they give to the observer is that of their "complexity." Some signals seem to vary more than others. Some appear extremely random while others seem to demonstrate a reappearance of certain patterns at various intervals. Indeed, in medical research signal variability or system complexity has been correlated with physiological conditions. Direct assessment of signal complexity/variability, thus, offers certain advantages in clinical research. First, complexity is an intuitive description and, thus, eases the interpretation of measurement results. Second, as mentioned, invariant measures allow comparison across different patient populations as they are insensitive to *absolute* measures such as amplitude and frequency.

Manuscript received January 10, 1997; revised April 10, 1998. The work of I. A. Rezek was supported by the European Community Commission, DG XII under Project SIESTA, Biomed-2 PL962 040. *Asterisk indicates corresponding author*.

*I. A. Rezek is with the Department of Electrical and Electronic Engineering, Imperial College of Science, Technology, and Medicine, Exhibition Road, London SW7 2BT, U.K. (e-mail: i.rezek@ic.ac.uk).

S. J. Roberts is with the Department of Electrical and Electronic Engineering, Imperial College of Science, Technology, and Medicine, London SW7 2BT, U.K.

Publisher Item Identifier S 0018-9294(98)06088-1.

II. CALCULATION OF COMPLEXITY

We have investigated four techniques which attempt to quantify signal complexity. We shall call these measures "complexity features," although the definition of "complexity" varies with each one of the feature extraction methods.

A. Autoregressive (AR) Model Order Estimation

Consider a deterministic system in which future samples are affected by a certain number of past samples. The number of past samples needed to predict the future sample may be regarded as a measure of complexity, as each such value will affect prediction difficulty and prediction uncertainty. If we use a linear prediction model, the model order can be considered a measure of complexity.

Methods of estimating AR models and model orders are described extensively in scientific literature [5]. In this study, we have used the standard Levinson–Durbin recursion to estimate AR parameters. The optimal model order was estimated using Akaike's final prediction error (FPE) [5], defined by $\mathrm{FPE}_p = \varepsilon_p(\frac{N+p+1}{N-p-1})$, where N is the number of data samples used, p the model order, and ε_p the prediction error power. If a large number of coefficients are required to model, then the sequence may be called "more complex" than one which requires only a few. We have, therefore, used the estimated optimum model order as an indicator of system complexity. It is worth noting that this complexity estimation will fail when the time sequence under observation may be regarded as random noise. In this case, model-order estimates will generally be low. This might be misinterpreted as a signal of 'low complexity" even though, intuitively, the opposite definition applies to noise. Also, the estimation relies on repetitive patterns found in the autocorrelation sequence. If such patterns do not exist, yet the sequence is not noise (e.g., a chaotic sequences), the model-order-estimation procedure will fail. In such cases, again, the estimated model order is too low.

B. Spectral Entropy

The next measure we introduce quantifies the spectral complexity of a time series. A variety of spectral transformations exist. Of these, the Fourier transformation (FT) [7] is probably the most well-known transformation method from which the power spectral density (PSD) $\hat{P}(f)$ can be obtained. The PSD $\hat{P}(f)$ is a density function, i.e., it represents the distribution of power as a function of frequency. Thus,

normalization of $\hat{P}(f)$, with respect to the total spectral power, will yield a probability density function (pdf). Application of Shannon's channel entropy gives an estimate of the spectral entropy (SE) of the process, where entropy is given as $H \equiv \sum_f p_f \log(1/p_f)$, and p_f is the pdf value at frequency f.

Heuristically, the entropy has been interpreted as a measure of uncertainty about the event at f. Thus, the entropy H may be used as a measure of system complexity. High uncertainty (entropy) is due to a large number of processes, whereas low entropy is due to a small number of dominating processes which make up the time series. Randomly distributed noise, for example, has high entropy values. In contrast, regular motions, such as sinusoids, give low entropy values. We note that spectral estimates are also easily obtained using parametric modeling techniques, in particular AR modeling. As we show empirically later in this paper, however, there is considerable uncertainty in the estimation of model order (which must be re-estimated over each time window in the signal). This fact, along with the undesirable property of AR models that noise and chaos induce a very low (but nonzero) model order, means that we choose FT-based methods for spectral estimation.

C. Approximate Entropy

In the field of nonlinear dynamics, complexity measures often statistically quantify the evolution of trajectory points in phase space. For instance, the Kolmogorov–Sinai (K-S) entropy [3] estimates the generation of information by computing the probabilities of nearby signal trajectory points remaining close after some time. However, most of these measures also aim to quantify chaotic sequences and, thus, require the use of limits (e.g., time $\rightarrow \infty$). The approximate entropy (ApEn) [10] also measures signal randomness. It does so without taking limits at the cost of being unable to detect chaos. It is, hence, more suitable for finite data sequences in which distinguishing chaos from high-complexity nonchaotic data is not of primary importance.

Consider the definition of the correlation sum [3]

$$C_i^m(r) = \frac{1}{N-m} \sum_{j=1}^{N-m} \Theta\big(r - \mathrm{norm}(\mathbf{u}_i, \mathbf{u}_j)\big) \tag{1}$$

where Θ is the Heaviside function and the norm may be defined in any consistent metric space. The parameter r corresponds to the distance within which neighboring trajectory points must lie (it is often referred to as bin size because of the correlation sum's correspondence to nonparametric pdf estimators). The vector $\mathbf{u}_i$ is the *embedding vector* [3] whose elements are m samples taken at intervals of J samples along the observed time series x, i.e., $\mathbf{u}_i = (x_i, x_{i+J}, \cdots, x_{i+(m-1)J})^T$. ApEn uses the correlation sum (1) as its basis [10], such that $\mathrm{ApEn}(m, r, N) = \Phi^{m+1}(r) - \Phi^m(r)$, where $\Phi^m = \log[P(\|\mathbf{u}_{j_m} - \mathbf{u}_{i_m}\| \leq r]$, i.e., the likelihood that m nearby points on the trajectory remain close to each other. Thus, ApEn measures the average conditional information generated by diverging points on the trajectory. The larger ApEn is the more complex than the signal. Noise causes ApEn to reach an upper bound.

D. Embedding Space Eigen Spectrum

The foundation of many quantitative methods in nonlinear dynamics is Taken's embedding theorem for noiseless systems [3, and references therein]. Using embedding vectors of the form $\mathbf{u}_i$ (as defined in the previous section), one can construct an embedding matrix $\mathbf{U}$, the column vectors of which are $\mathbf{u}_1^T, \mathbf{u}_1^T, \cdots, \mathbf{u}_{N-(i-1)}^T$ constructed from N time-series samples. The value m is referred to as the *embedding dimension* and must satisfy Taken's Theorem $m \geq 2M + 1$, which sets the lower bound for m given an M-dimensional manifold in the phase space [1]. Since M is not known *a priori*, the embedding dimension m is chosen large enough so that redundancy results. This leads to a rank deficiency of the embedding matrix $\mathbf{U}$ and, therefore, some of the eigenvalues σ_i^2 of $\mathbf{U}^T\mathbf{U}$ will be zero. It was shown in [1] that the rank is an upper bound to the trajectory dimension, and we utilize a measure of this as an alternative estimate of system complexity.

In real-world situations, the observed time series will be corrupted by experimental noise (including quantization noise). This, as shown in [1], results in a shifting of the eigenvalues, such that $\sigma_i^2 \rightarrow \sigma_i^2 + \langle \xi^2 \rangle$, where $\langle \xi^2 \rangle$ is the expected signal noise variance. Hence, no eigenvalue will be zero. There will be a spread of significant eigenvalue "power" away from the first singular values, if the trajectory is of larger dimension. We quantify this spread using the fractional spectral radius (FSR), defined as $\mathrm{FSR}(j) = (\sum_{i=0}^{j} \sigma_i^2)/(\sum_{l=0}^{m} \sigma_l^2)$. The value of j was empirically set to $j = 1$, i.e., only the first eigenvalue was used. A trajectory which is spanned by a higher number of independent variables is considered more complex (as more information is required to specify the state of the system) and is characterized by a low FSR value. A value of FSR close to unity indicates a system with a very low number of degrees of freedom and, thus, low complexity.

III. Simulation

The behavior of all four complexity measures is first demonstrated using the logistic map [3]

$$x_{n+1} = R x_n (1 - x_n) \tag{2}$$

where the parameter R determines the regime of oscillation produced by the map. If R is set in the range of $0 \leq R \leq 4$, the series x_n will demonstrate period-doubling phenomena and, eventually, chaotic oscillations at $R = 3.6$ [3].

We do not propose the logistic-map model as a model for any biological system. It has pragmatically been chosen here for reasons of comparability with the literature [10], and as it is well known [3]. In addition, it is a one-dimensional system which does not require numerical integration to obtain an output. The number of control parameters is, hence, kept to a minimum.

Table I shows the values obtained for each of the complexity measures, based on 512 samples, for the different oscillatory regimes of the logistic map (as determined by R). SE clearly increases as the map bifurcates further and further. The highest SE values are found when the map is chaotic. Similar observations can be made for AR model-order estimates. However, the actual estimated values for the order do not correspond to the period number of (2). Note also that in the chaotic regime, i.e., for a very complex time-series, estimated model orders are very low. Similar estimates result if an AR process is used to model a random noise signal. Although AR model estimation may be a simple tool for complexity measurements, it is nonetheless ambiguous. Signals of low complexity and noise cannot be distinguished by this method. ApEn results are shown based on distance bins (r) of approximately 0.1 standard deviations of $\{x\}$ in size. The more complex the dynamic behavior of the system becomes, the more ApEn increases. However, as pointed out in [10], the function is very sensitive to the width of the distance bins. FSR measures show a consistent decrease with R, indicating signals of increasing complexity.

IV. Physiological Signal Analysis

We first present examples of complexity analysis applied to electroencephalogram (EEG) and respiratory recordings of a patient

TABLE I
COMPLEXITY ESTIMATES FOR LOGISTIC MAP WITH DIFFERENT VALUES OF R

Logistic Map Parameter R	3.2	3.48	3.56	3.568	3.57	3.8
Spectral Entropy	0.86	1.02	1.25	1.26	1.27	5.17
AR Model Order	2	8	14	18	18	3
Fractional Spectral Radius	0.99	0.80	0.63	0.59	0.58	0.11
Approximate Entropy	$9.6E-06$	$1.35E-05$	$2.15E-05$	0.0893	0.0894	0.4981

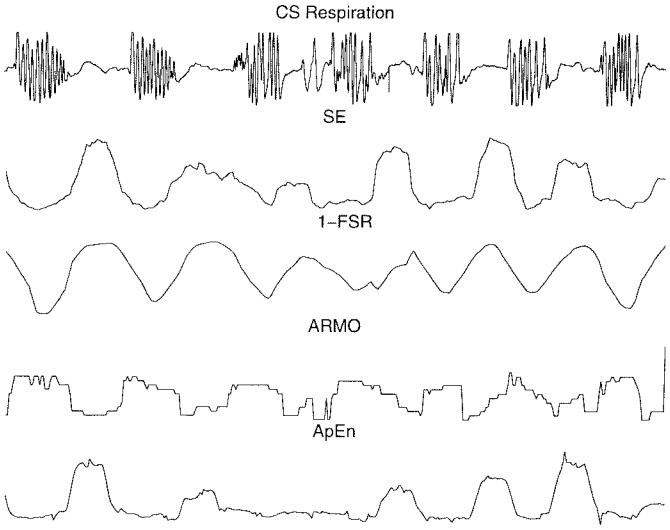

Fig. 1. Complexity measures during CS respiration movements.

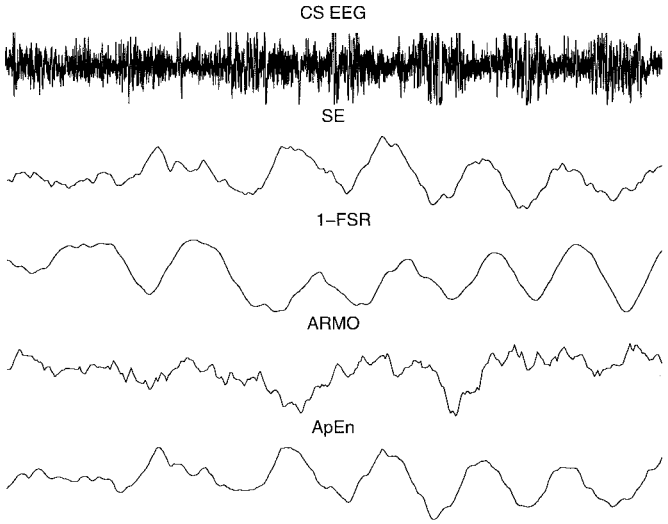

Fig. 2. Complexity measures during CS EEG; same time segment as in Fig. 1.

during Cheyne–Stokes (CS) respiration and on EEG recordings from patients during anesthesia.

EEG recordings were sampled at 128 Hz and, subsequently, low-pass filtered using an 11th-order finite-impulse-response filter with a cutoff frequency of 25 Hz. Consecutive overlapping windows were taken, and data within each were subject to the analysis of all four feature extraction methods. Window length was set to 4 s, with a window overlap of 75%. The resulting feature values were then filtered using a 10th-order moving-average boxcar filter, with the exception of AR model-order estimates which were filtered with an 11th-order moving-median filter.

Figs. 1 and 2 show the time course of the feature values together with the corresponding respiration and EEG recordings for a duration of approximately 6.5 min. Respiration shows alternating epochs of apnoea and respiration movements (hyper-ventilation/apnoea) typical of CS breathing. All features show changes corresponding to respiratory periodicity. During apnoea, FSR decreases, as the trajectory constitutes mainly noise (Note that we have plotted 1-FSR for illustrative purposes only and as lower values of this correspond to reduced "complexity"). Similarly, AR model-order estimates are low, indicating little to be modeled but noise. Because noise resembles high uncertainty, both entropy estimates (SE and ApEn) are high as compared to estimates during respiratory activity. The more interesting result (Fig. 2) is that features obtained from the EEG recording also demonstrate changes which correspond to changes in respiration, i.e., information regarding the respiratory state is also contained in the EEG recordings themselves. As was seen in the respiratory analysis, a clear periodic structure is evident in all complexity measures with the exception of AR model-order estimation.

All four "complexity" methods were also applied to EEG recordings obtained from patients during anesthesia. Anesthetic levels were

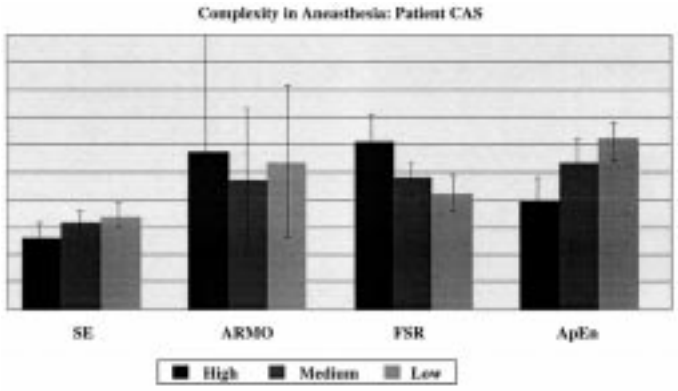

Fig. 3. Complexity changes in the EEG for differing depth of anesthesia.

determined by the concentration of anesthetic agent given to the subjects (see [6] for further details). Fig. 3 shows the results for low, medium, and high levels of anesthetic agent concentration. Low levels of anesthetic agent concentration correspond to low depth of anesthesia, and vice versa. The results clearly show a reduction in SE with increased depth of anesthesia. Similarly, FRS increases as the first eigenvalue accounts, increasingly, for a larger part of the spectral radius. Again, ApEn follows closely the results obtained from SE, however, with apparently higher sensitivity and reduced error. AR model-order estimation failed completely to distinguish between any of the three levels (note the very large error bars). This was in line with the results obtained from the CS EEG data and simulation, but opposed to some researchers who have used AR model-order estimation successfully in EEG analysis [8], although conclusions drawn from just one data set must be taken with care.

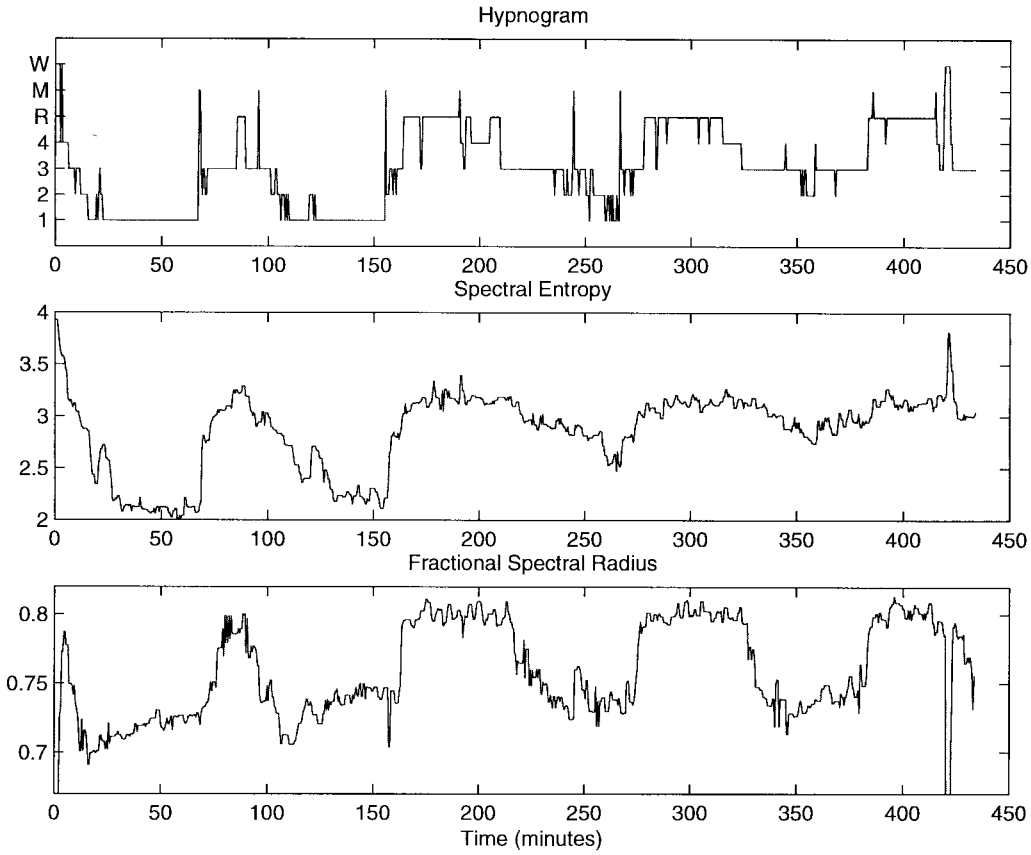

Fig. 4. Complexity measures of sleep EEG recording.

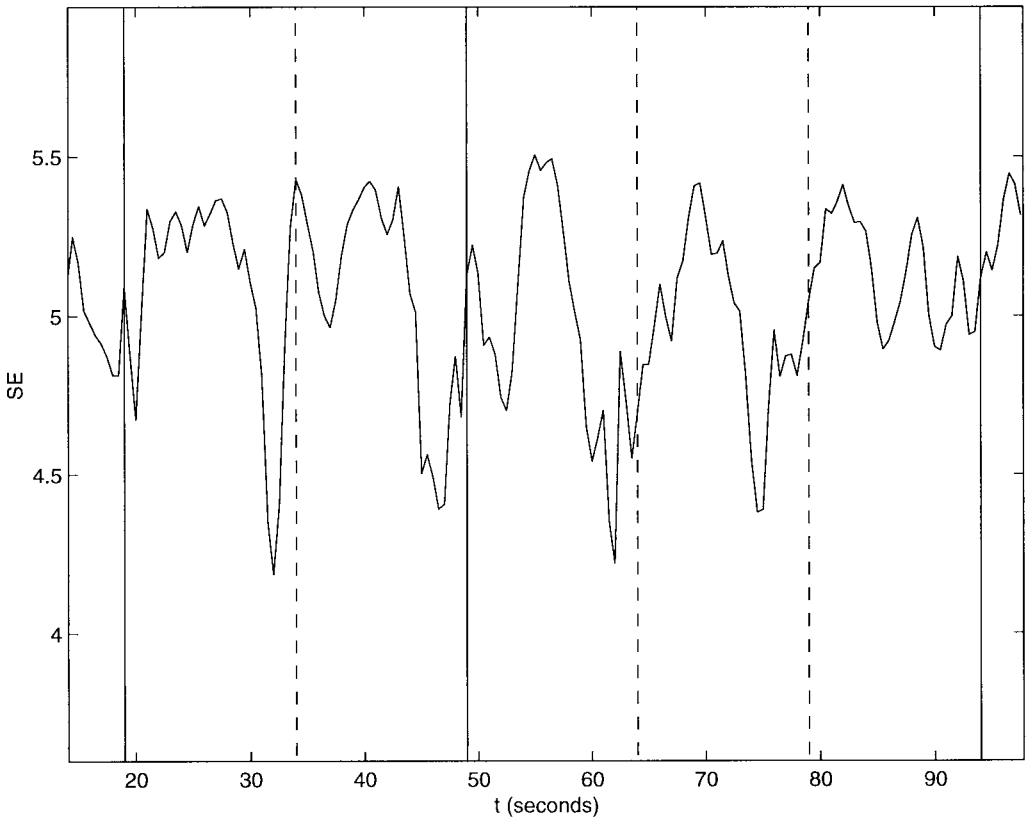

Fig. 5. SE for imagined finger movement EEG recording. Solid and dashed lines indicate right and left imagined movements, respectively.

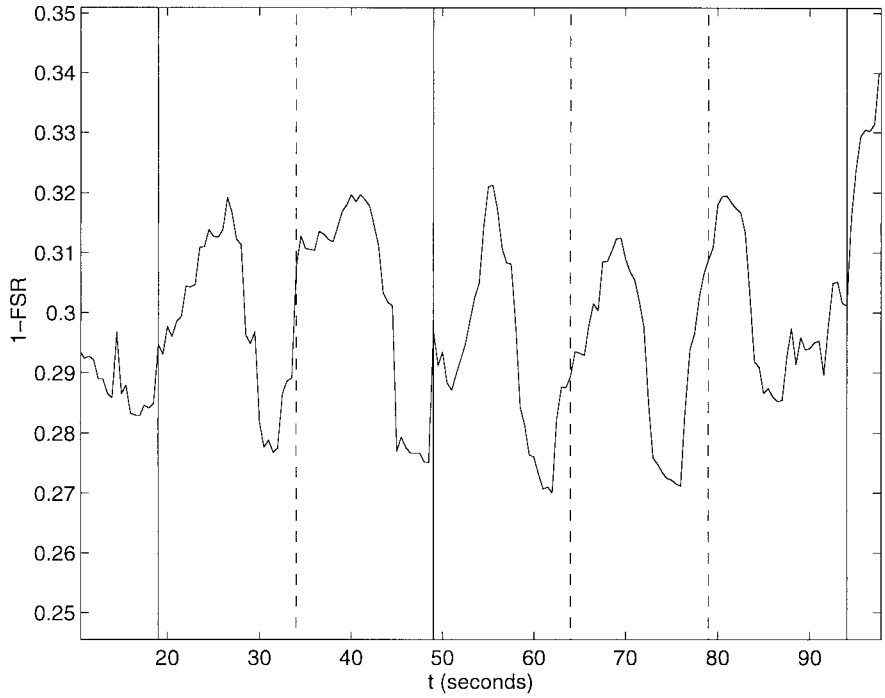

Fig. 6. Fractional spectral radius (1-FSR) for imagined finger movement EEG recording.

Fig. 4 shows the estimates of SE and FSR applied to a 7-h-sleep EEG recording. The manually scored EEG sleep stages are shown in the hypnogram trace (levels W, M, R, 1, 2, 3, and 4 correspond to wakefulness, movement, REM and sleep stages 1, 2, 3 and 4, respectively, on a 30-s resolution). The complexity measures compare favorably with the hypnogram.

Our final example is an application of complexity measures to EEG recordings obtained from subjects during imagined finger movements. These recordings form part of a wider "brain-computer interface" project designed to detect and classify imagined limb movements from EEG recordings. Fig. 5 and 6 depict the SE and FSR values, calculated over 2-s sliding windows with 75% overlap, together with the event times of the imagined finger movement cues (vertical lines) for a typical recording fragment. Both measures exhibit a clear reduction in complexity prior to the movement. This is consistent with the notion of movement-planning changes in the EEG, as discussed in [9]. We note that no filtering was performed on the complexity traces.

V. Discussion

There are various definitions of complexity, four of which are addressed by the feature-extraction methods presented in this paper. Of these methods, SE, ApEn, and FSR have performed well. In particular, their sensitivity to levels of anesthetic agent indicates their usefulness as features for such problems (see [6]). In this respect, they may succeed where other methods have failed [12]. AR model-order estimation failed to give satisfactory results for the EEG signals used in this paper. This appears to be independent of the AR parameter estimation method and the model order criterion. The combination of Yule–Walker and FPE gives highest sensitivity, however. Other methods, such as Burg's method, in conjunction with FPE, were found to be less sensitive and the resultant complexity measures even more erratic. In all of the above examples, the sampling frequency was kept constant when comparing the complexity features for different signals. Clearly, in the case of SE, the sampling frequency is crucial and will affect the SE estimates. For instance, increase in sampling frequency will naturally increase the SE estimates. Similarly, sampling affects the AR model-order estimates, as well as FSR and ApEn. Particularly in the case of FSR, an additional parameter, the embedding dimension, is also crucial in determining the resolution of the complexity measure. To detect faster changes, smaller embedding dimensions must be chosen and vice versa [2].

Other complexity measures have been proposed, such as Hjorth coefficients [4], number of zero crossings, and many more in the field of nonlinear dynamics. Many of these measures are related. Clearly, the number of zero crossings is related to spectral estimation methods and, thus, in some respect, to SE. Hjorth coefficients are measures of low-order spectral moments and are related to the spectral entropy for systems with a dominant spectral peak.

Clearly, all methods can be improved upon. Spectral leakage and windowing have an effect on the SE estimates. For instance, a single oscillation whose frequency is incommensurate with the sampling frequency will result in higher SE estimates. On the other hand, temporal smoothing with a window function causes the SE estimates to decrease. Recent work concerning a Bayesian analysis of singular value decomposition [11] is closely related to our FSR measure and a Bayesian approach to complexity estimation is an area for future research.

Acknowledgment

The authors would like to thank Dr. J. Stradling and Dr. R. Davies of the Osler Chest Unit at the Churchill Hospital, Oxford, U.K., and Dr. C. Jordan of the Academic Department of Anesthesia at the Northwick Park Hospital, Harrow, U.K. They would also like to thank the anonymous reviewers for their valuable feedback. They would like further to thank Dr. M. Stokes at the Royal Hospital for Neurodisability, Putney, U.K., and the Living Again Trust.

References

[1] D. S. Broomhead and G. P. King, "Extracting qualitative dynamics from experimental data," *Physica D*, vol. 20, pp. 217–236, 1986.

[2] J. B. Elsner and A. A. Tsonis, *Singular Spectrum Analysis: A New Tool in Time Series Analysis*. New York: Plenum, 1996.
[3] R. C. Hilborn, *Chaos and Nonlinear Dynamics*. New York: Oxford Univ. Press, 1994.
[4] B. Hjorth, "EEG analysis based on time domain properties," *Electroencephalogr., Clin, Neurophysiol.*, vol. 29, pp. 306–310, 1970.
[5] S. M. Kay and S. L. Marple, "Spectrum analysis—A modern perspective," *Proc. IEEE*, vol. 69, pp. 1380–1419, Nov. 1981.
[6] M. Krkic, S. J. Roberts, I. A. Rezek, and C. Jordan, "EEG-based assessment of anaesthetic-depth using neural networks," in *Proc. Inst. Elect. Eng. AI Methods in Biosignal Analysis*, Apr. 1996, pp. 10/1–10/6.
[7] S. L. Marple, *Digital Spectral Analysis with Applications*. Englewood Cliffs, NJ: Prentice-Hall, 1987.
[8] J. Pardey, S. J. Roberts, and L. Tarassenko, "A review of parametric modeling techniques for EEG analysis," *Med. Eng., Phys.*, vol. 18, no. 1, pp. 2–11, 1996.
[9] G. Pfurtscheller, D. Flotzinger, and C. Neuper, "Differentiation between finger, toe, and tongue movement in man based on 40-Hz EEG," *Electroencephalogr., Clin. Neurophysiol.*, vol. 90, pp. 456–460, 1994.
[10] S. M. Pincus, "Approximate entropy as a measure of system complexity," in *Proc. National Academy of Science USA*, vol. 88, pp. 2297–2301, Mar. 1991.
[11] J. J. Rajan and P. J. W. Rayner, "Model order selection for singular value decomposition and the discrete Karhunen–Loève transform using a Bayesian approach," in *Proc. Inst. Elect. Eng, Vision, Image, and Signal Processing*, 1997, vol. 144, no. 2, pp. 116–123.
[12] H. U. Rehman, D. A. Linkens, and A. J. Asbury, "Neural networks and nonlinear regression modeling and control of depth of anaesthesia for spontaneously breathing and ventilated patients," *Comput. Meth., Programming in Biomed.*, vol. 40, pp. 227–247, 1993.